# Quantum Nondemolition Measurement of a Quantum Squeezed State Beyond the 3 dB Limit

C. U. Lei, A. J. Weinstein, J. Suh, E. E. Wollman, A. Kronwald, F. Marquardt, A. A. Clerk, and K. C. Schwab

Phys. Rev. Lett. **117**, 100801 — Published 30 August 2016

DOI: 10.1103/PhysRevLett.117.100801

# Quantum nondemolition measurement of mechanical squeezed state beyond the 3 dB limit

C. U. Lei,[1] A. J. Weinstein,[1] J. Suh,[2] E. E. Wollman,[1] A. Kronwald,[3,4] F. Marquardt,[3,4] A. A. Clerk,[5] K. C. Schwab[1*]
[1] *Applied Physics, California Institute of Technology, Pasadena, CA 91125, USA*
[2] *Korea Research Institute of Standards and Science, Daejeon 305-340, Republic of Korea*
[3] *Friedrich-Alexander-Universität Erlangen-Nürnberg, Staudtstr. 7, D-91058 Erlangen, Germany*
[4] *Max Planck Institute for the Science of Light Günther-Scharowsky-Straße 1/Bau 24, D-91058 Erlangen, Germany and*
[5] *Department of Physics, McGill University, Montreal, Quebec, H3A 2T8 Canada*
(Dated: August 11, 2016)

We use a reservoir engineering technique based on two-tone driving to generate and stabilize a quantum squeezed state of a micron-scale mechanical oscillator in a microwave optomechanical system. Using an independent backaction evading measurement to directly quantify the squeezing, we observe $4.7 \pm 0.9$ dB of squeezing below the zero-point level, surpassing the 3 dB limit of standard parametric squeezing techniques. Our measurements also reveal evidence for an additional mechanical parametric effect. The interplay between this effect and the optomechanical interaction enhances the amount of squeezing obtained in the experiment.

Generating nonclassical states of a massive object has been a subject of considerable interest. It offers a route toward fundamental tests of quantum mechanics in an unexplored regime [1]. One of the most important and elementary quantum states of an oscillator is a squeezed state [2], which is a minimum uncertainty state has a quadrature which is smaller than the zero-point level. Such states have long been discussed in the context of gravitational wave detection to improve the measurement sensitivity [3–5]. It is well known that a coherent parametric drive can be used to squeeze mechanical fluctuations [6, 7], which is essentially equivalent to the technique first used to squeeze ground-state optical fields [8]. However, the maximum steady-state squeezing achieved by this method is limited to 3 dB due to the onset of parametric instability. Therefore, it is in principle impossible to have a steady state where the mechanical motion is squeezed below one half of the zero-point level using only parametric driving. These limitations may be overcome by combining continuous quantum measurement and feedback [9–12], but it would substantially increase the experimental complexity.

Another method to generate robust quantum state is quantum reservoir engineering [13], which has been used to generate quantum squeezed states and entanglement with trapped ions [14, 15] and superconducting qubits [16]. It can also applied to optomechanical system to generate strong steady-state squeezing without quantum-limited measurement and feedback [17]. By modulating the optomechanical coupling with two imbalanced classical drive tones, the driven cavity acts effectively as a squeezed reservoir. When the engineered dissipation from the cavity dominates the dissipation from the environment, the mechanical resonator relaxes to a steady squeezed state. This technique has been applied recently to generate quantum squeezed states of macroscopic mechanical resonators [18–20].

In addition to being a tool for state preparation, optomechanics also provides a means to probe the quantum behavior of macroscopic objects [21–23]. In particular, a backaction evading (BAE) measurement [10, 20, 24–27] of a single motional quadrature can be implemented in an optomechanical system. If the drive tones that modulate the coupling are balanced, a continuous quantum nondemolition (QND) measurement of the mechanical quadrature can be made. This technique can be used to fully reconstruct the quantum state of the mechanical motion.

In this work, we combine reservoir engineering and backaction evading measurement with a microwave optomechanical system to perform continuous QND measurement of a quantum squeezed state. Among the previous three squeezing experiments [18–20], only [20] demonstrated direct detection, performed using a two-cavity optomechanical system; here we implement both reservoir engineering and BAE measurement simultaneously within a simple single-cavity setup. In addition to the optomechanical interaction, a mechanical parametric effect is observed. Contrary to previous works, where the mechanical parametric effect produced parametric instability that limited the precision of the BAE measurement [26, 28, 29], the interplay between the parametric drive and the engineered dissipation enhances the mechanical squeezing. By directly measuring the mechanical quadrature variances with the BAE measurement, we demonstrate motional quantum squeezing with squeezed quadrature variance $\langle \Delta X_1^2 \rangle = 0.34 \pm 0.07 x_{\rm zp}^2$, $4.7 \pm 0.9$ dB below the zero-point level. This exceeds what is possible using only parametric driving, even if one starts in the quantum ground state. This is the first experiment to demonstrate more than 3 dB quantum squeezing in a macroscopic mechanical system.

The mechanical oscillator in this work is a 100 nm thick, $40 \times 40\,\mu\text{m}^2$ aluminum membrane, with fundamental resonance frequency $\omega_m = 2\pi \times 5.8$ MHz and mechanical linewidth $\Gamma_m = 2\pi \times 8$ Hz at 10 mK. It is capacitively coupled to a lumped-element superconducting microwave

resonator with resonance frequency $\omega_c = 2\pi \times 6.083$ GHz and damping rate $\kappa = 2\pi \times 330$ kHz (Fig. 1a). The mechanical motion couples to the resonance frequency of the microwave resonator through the modulation of the capacitance, with an optomechanical coupling rate $g_0 = \frac{d\omega_c}{dx} x_{\rm zp} = 2\pi \times 130$ Hz, where $x_{\rm zp} = \sqrt{\frac{\hbar}{2m\omega_m}} = 1.8$ fm is the amplitude of the zero-point fluctuation of the mechanical oscillator with mass $m = 432$ pg. The system is described by the Hamiltonian

$$\hat{H} = \hbar\omega_c \hat{a}^\dagger \hat{a} + \hbar\omega_m \hat{b}^\dagger \hat{b} - \hbar g_0 \hat{a}^\dagger \hat{a} \left(\hat{b} + \hat{b}^\dagger\right) + i\hbar\sqrt{\kappa_{\rm in}}(\alpha^*(t)\hat{a} - \alpha(t)\hat{a}^\dagger) + \hat{H}_{\rm diss}, \quad (1)$$

where $\hat{a}$ $(\hat{a}^\dagger)$ is the annihilation (creation) operator of the intra-cavity field, $\hat{b}$ $\left(\hat{b}^\dagger\right)$ is the mechanical phonon annihilation (creation) operator, $\kappa_{\rm in}$ is the coupling rate of the input coupler, and $\alpha(t)$ is the external driving field. The term $\hat{H}_{\rm diss}$ accounts for dissipation.

To squeeze the mechanical motion, we drive the cavity with a pair of pump tones at $\omega_c \mp \omega_m$ with intracavity field [17]

$$\bar{\alpha}_{\rm sqz}(t) = (\bar{\alpha}_- e^{i\omega_m t} + \bar{\alpha}_+ e^{-i\omega_m t}) e^{-i\omega_c t}, \quad (2)$$

which is represented by the red and blue arrows in Fig. 1b. Linearizing the cavity dynamics in the standard way, the pumps couple the microwave resonator to the Bogoliubov mode of the mechanical motion with the Hamiltonian

$$\hat{H}_{\rm sqz} = -\hbar\mathcal{G}(\hat{d}^\dagger \hat{\beta} + \hat{d}\hat{\beta}^\dagger), \quad (3)$$

where $\hat{d}$ is the fluctuating part of the cavity field $\hat{a}$, and $\hat{\beta} = \hat{b}\cosh r + \hat{b}^\dagger \sinh r$ is the Bogoliubov-mode annihilation operator whose ground state is a squeezed state with squeezing parameter $r = \tanh^{-1}(G_+/G_-)$. $\mathcal{G} = \sqrt{G_-^2 - G_+^2}$ is the coupling rate between the Bogoliubov mode and the cavity. $G_\mp = g_0\sqrt{n_p^\mp}$ are the enhanced optomechanical coupling rates, and $n_p^\mp = |\bar{\alpha}_\mp|^2$ are the intracavity pump photon numbers corresponding to the squeezing pumps. The beam-splitter Hamiltonian in Eq. (3) enables us to cool the Bogoliubov-mode into its ground state, producing a stationary mechanical squeezed state with quadrature variances

$$\langle \Delta \hat{X}_{1,2}^2 \rangle = x_{zp}^2 \left\{ \frac{\Gamma_m}{\Gamma_{\rm eff}} \left(2n_m^{th} + 1\right) + \frac{\Gamma_{\rm opt}^\mp}{\Gamma_{\rm eff}} \left(2n_c^{th} + 1\right) \right\}, \quad (4)$$

where $\Gamma_{\rm eff} = \Gamma_m + 4\mathcal{G}^2/\kappa$ is the effective mechanical linewidth and $\Gamma_{\rm opt}^\mp = 4(G_- \mp G_+)^2/\kappa$ parameterizes the phase-dependent driving of the mechanics by cavity fluctuations.

To extract the mechanical quadrature variance, we measure the normalized noise spectra of the cavity resonance (the lower inset in Fig. 1f(g)) and the mechanical sideband (the upper inset in Fig. 1f(g)). By fitting the normalized spectra with the optomechanical model [30], we can extract the cavity occupation $n_c^{\rm th}$ and the phonon bath occupation $n_m^{\rm th}$. Together with the calibrations of the enhanced optomechanical coupling rate $G_\pm$, we can calculate the quadrature variances with Eq. (4) [17, 18].

Fig. 1c shows the quadrature variances with various intracavity pump photon ratio $n_p^+/n_p^-$. We start by squeezing the mechanical motion with total intracavity pump photon number $n_p^{\rm tot} = n_p^- + n_p^+ = 1.35 \times 10^4$ and pump photon ratio $n_p^+/n_p^- = 0.5$. This pump configuration generates a mechanical squeezed state with the squeezed quadrature variance $\langle \Delta \hat{X}_1^2 \rangle = 1.54 \pm 0.59 x_{\rm zp}^2$ and the anti-squeezed quadrature variance $\langle \Delta \hat{X}_2^2 \rangle = 13.8 \pm 1.4 x_{\rm zp}^2$, indicated by the solid red circle and square in Fig. 1c. The corresponding normalized output spectra and the fits from the two-tone optomechanical model [17] are shown in Fig. 1f. To further squeeze the mechanical motion, we can increase the total pump photon number. The blue circles (squares) in Fig. 1c are the squeezed (anti-squeezed) quadrature variances at total intracavity pump photon number $n_p^{\rm tot} = 1.85 \times 10^5$. The solid (dashed) blue curves are the predictions from Eq. (4) with constant cavity and mechanical occupations extracted from the output spectrum at $n_p^+ = 0$; they agree with the data at low pump photon ratio. At large pump photon ratio, the cavity bath starts to heat up (Fig. 1d), which increases the mechanical quadrature variances. The orange curves in Fig. 1c are the predictions from Eq. (4) including the cavity heating effect extracted from the experiment (orange line in Fig. 1d). With the heating effect, the minimum quadrature variance is achieved at $n_p^+/n_p^- = 0.43$ with $\langle \Delta \hat{X}_1^2 \rangle = 0.56 \pm 0.02 x_{\rm zp}^2$ (the solid blue circle in Fig. 1d), $2.5 \pm 0.2$ dB below the zero-point level. The corresponding normalized output spectra and fits are shown in Fig. 1g.

While inferring the level of squeezing from the cavity output spectrum is convenient, it would be preferable to have a more direct method that does not rely on assumptions about the mechanical dynamics. This can be achieved in our system without needing to introduce an additional cavity resonance: we continue to use the cavity density of states near resonances to generate mechanical squeezing, but now use the density of states away from resonances to make an independent, backaction-evading measurement of a single mechanical quadrature. In this way, our single cavity effectively plays the role of two: it both generates squeezing, and permits an independent detection of the squeezing.

To directly measure a single mechanical quadrature, in addition to the squeezing pumps, we introduce another pair of weak backaction evading (BAE) probes (the purple arrows in Fig. 1b) at $\omega_c \mp \omega_m - \Delta$ with intracavity field [18, 27]

$$\bar{\alpha}_{\rm BAE}(t) = 2\bar{\alpha}\cos(\omega_m t + \phi) e^{-i(\omega_c - \Delta)t}, \quad (5)$$

where $\phi$ is the relative phase between the BAE probes and the squeezing pumps. For a sideband-resolved system ($\omega_m \gg \kappa$), the modulation of the BAE probes exclusively couples the mechanical quadrature $\hat{X}_\phi = \cos\phi\hat{X}_1 - \sin\phi\hat{X}_2$ to the microwave resonance with the interaction

$$\hat{H}_I = -\hbar G(\hat{d}^\dagger e^{-i\Delta t} + \hat{d}e^{i\Delta t})\frac{\hat{X}_\phi}{x_{\rm zp}}, \tag{6}$$

where $G = g_0\sqrt{n_p}$ is the enhanced optomechanical coupling rate and $n_p = |\bar{\alpha}|^2$ is the intracavity pump photon number corresponding to the BAE probes. Since $\hat{X}_\phi$ is a constant of motion of the system, the interaction (6) enables a continuous QND measurement of the the mechanical quadrature. By sweeping the probe phase $\phi$, we can perform tomography of the mechanical quantum state (Fig. 2a). In order to ensure no interference between the sidebands of the squeezing pumps and the BAE probes, we detune the BAE sidebands from the cavity resonance by $\Delta = 2\pi \times 160\text{kHz} \gg \Gamma_{\rm eff}$. The power of the BAE probes are set about 10 dB weaker than the power of the squeezing pumps to avoid extra heating. In the experiment, the motional sideband spectrum of the BAE probes is measured, from which we can extract the mechanical quadrature variance and linewidth. In the following, we will perform a BAE measurement to directly characterize the weakly squeezed state corresponding to the spectrum Fig. 1f and the strong squeezed state corresponding to the spectrum Fig. 1g.

Fig. 2b shows the mechanical quadrature variance as a function of the probe phase $\phi$. The red circles are the quadrature variances of the weakly squeezed state measured with the BAE technique. The red curve is the quadrature variance inferred from the corresponding output spectrum (Fig. 1f). In this case, the results from the BAE measurement are in good agreement with the results inferred from the output spectra. Similarly, the blue circles are the quadrature variances of the strong squeezed state measured with the BAE technique. The blue curve is the quadrature variance inferred from the corresponding output spectra (Fig. 1g). The minimum quadrature variance is achieved at $\phi = 0°$ with $\langle\Delta\hat{X}_\phi^2\rangle = 0.34 \pm 0.07 x_{\rm zp}^2$, $4.7 \pm 0.9$ dB below the zero-point level. This is lower than the quadrature variance inferred from the output spectrum, implying that there is additional dynamics at play (beyond the ideal optomechanical interaction).

The enhanced squeezing observed in the BAE measurement suggests an additional squeezing mechanism beyond the dissipative mechanism discussed above; an obvious candidate is direct parametric driving of the mechanics. The presence of such driving is further corroborated by our observation of a phase dependence of the quadrature linewidth in the BAE measurement (Fig. 2c). Similar induced mechanical parametric driving has been observed in other BAE measurements; they can arise via a number of mechanisms, including thermal effects as well as higher nonlinearities [28, 29]. To understand the effects of this mechanical parametric driving, we phenomenologically add the mechanical parametric interaction to our otherwise ideal optomechanical model [30]:

$$\hat{H}_{\rm para} = -\hbar\lambda(e^{i\psi}\hat{b}^2 + e^{-i\psi}\hat{b}^{\dagger 2}), \tag{7}$$

where $\lambda$ is the amplitude of the parametric interaction and $\psi$ is the relative phase between the parametric drive and the squeezing pumps.

We fit the observed phase-dependent quadrature linewidth to our model, thus extracting the amplitude and phase of the parametric drive. [30]. By assuming the phase of the parametric drive $\psi$ follows the phase of the BAE probe (i.e. $\psi = \phi + \psi_0$, where $\psi_0$ is a constant phase shift), the model captures the observed phase dependence behavior of the quadrature linewidth, as shown by the dashed curves in Fig. 2c. Surprisingly, if one instead assumes that the parametric driving is a result of the main squeezing tones (i.e. take $\psi$ a constant independent of $\phi$), one cannot capture the observed phase dependence of the quadrature linewidth [30]. These results suggest that the parametric drive is induced by the BAE probes.

The dashed curves in Fig. 2b are the predicted quadrature variance including the mechanical parametric effect. The model suggests that the combination of the reservoir engineering with the mechanical parametric drive provide extra squeezing. However, the model doesn't fully capture the observed quadrature variance in the BAE measurement. The deviation may be due to the complicated heating effects associated with the underlaying nonlinearities [28, 29] that cause the spurious mechanical parametric drive. We stress that our treatment of the spurious mechanical parametric drive is phenomenological; we do not know the precise microscopic mechanism which causes this driving. Nonetheless, it allows us to explain both surprising features of the BAE measurements (the observed phase-dependent mechanical quadrature linewidth, and the enhanced squeezing), and provide a direction to engineer the parametric drive to increase the squeezing [30].

In conclusion, we combine reservoir engineering and backaction evading measurement in a microwave optomechanical system to demonstrate a continuous QND measurement of mechanical squeezed states. A spurious mechanical parametric effect is observed and provide additional squeezing. Together with the spurious mechanical parametric drive, the reservoir engineering technique produce more than 3 dB squeezing below the zero-point level. The present scheme can be applied to generate and characterize more complicated quantum states by carefully engineering the nonlinear interaction [31, 32]. The ability to generate and measure a strong quantum squeezed

state of a macroscopic mechanical object would be useful for ultra-sensitive detection [3], quantum information processing [33], as well as fundamental study of quantum decoherence [34, 35].

This work is supported by funding provided by the Institute for Quantum Information and Matter, an NSF Physics Frontiers Center with support of the Gordon and Betty Moore Foundation (NSF-IQIM 1125565), by the Defense Advanced Research Projects Agency (DARPA-QUANTUM HR0011-10-1-0066), by the NSF (NSF-DMR 1052647 and NSF-EEC 0832819), and by the Semiconductor Research Corporation (SRC) and Defense Advanced Research Project Agency (DARPA) through STARnet Center for Function Accelerated nanoMaterial Engineering (FAME). J.S was supported by Basic Science Research Program through the National Research Foundation of Korea(NRF) funded by the Ministry of Science, ICT & Future Planning (2016R1C1B2014713 and 2016R1A5A1008184). A.C., F.M., and A.K. acknowledge support from the DARPA ORCHID program through a grant from AFOSR, F.M. and A.K. from ITN cQOM and the ERC OPTOMECH, and A.C. from NSERC.

* schwab@caltech.edu

[1] M. Aspelmeyer, P. Meystre, and K. Schwab, Phys. Today **65**, 29 (2012).
[2] D. Stoler, Phys. Rev. D **1**, 3217 (1970).
[3] J. N. Hollenhorst, Phys. Rev. D **19**, 1669 (1979).
[4] C. M. Caves, K. S. Thorne, R. W. P. Drever, V. D. Sandberg, and M. Zimmermann, Rev. Mod. Phys. **52**, 341 (1980).
[5] C. M. Caves, Phys. Rev. D **23**, 1693 (1981).
[6] M. P. Blencowe and M. N. Wybourne, Physica B (Amsterdam) **280**, 555 (2000).
[7] D. Rugar and P. Grütter, Phys. Rev. Lett. **67**, 699 (1991).
[8] L.-A. Wu, H. J. Kimble, J. L. Hall, and H. Wu, Phys. Rev. Lett. **57**, 2520 (1986).
[9] R. Ruskov, K. Schwab, and A. N. Korotkov, Phys. Rev. B **71**, 235407 (2005).
[10] A. A. Clerk, F. Marquardt, and K. Jacobs, New J. Phys. **10**, 095010 (2008).
[11] A. Szorkovszky, A. C. Doherty, G. I. Harris, and W. P. Bowen, Phys. Rev. Lett. **107**, 213603 (2011).
[12] A. Szorkovszky, G. A. Brawley, A. C. Doherty, and W. P. Bowen, Phys. Rev. Lett. **110**, 184301 (2013).
[13] F. Verstraete, M. M. Wolf, and J. Ignacio Cirac, Nat. Phys. **5**, 633 (2009).
[14] Y. Lin, J. P. Gaebler, F. Reiter, T. R. Tan, R. Bowler, A. S. Sørensen, D. Leibfried, and D. J. Wineland, Nature (London) **504**, 415 (2013).
[15] D. Kienzler, H.-Y. Lo, B. Keitch, L. de Clercq, F. Leupold, F. Lindenfelser, M. Marinelli, V. Negnevitsky, and J. P. Home, Science **347**, 53 (2015).
[16] S. Shankar, M. Hatridge, Z. Leghtas, K. M. Sliwa, A. Narla, U. Vool, S. M. Girvin, L. Frunzio, M. Mirrahimi, and M. H. Devoret, Nature (London) **504**, 419 (2013).
[17] A. Kronwald, F. Marquardt, and A. A. Clerk, Phys. Rev. A **88**, 063833 (2013).
[18] E. E. Wollman, C. U. Lei, A. J. Weinstein, J. Suh, A. Kronwald, F. Marquardt, A. A. Clerk, and K. C. Schwab, Science **349**, 952 (2015).
[19] J.-M. Pirkkalainen, E. Damskägg, M. Brandt, F. Massel, and M. A. Sillanpää, Phys. Rev. Lett. **115**, 243601 (2015).
[20] F. Lecocq, J. B. Clark, R. W. Simmonds, J. Aumentado, and J. D. Teufel, Phys. Rev. X **5**, 041037 (2015).
[21] A. J. Weinstein, C. U. Lei, E. E. Wollman, J. Suh, A. Metelmann, A. A. Clerk, and K. C. Schwab, Phys. Rev. X **4**, 041003 (2014).
[22] J. D. Cohen, S. M. Meenehan, G. S. MacCabe, S. Gröblacher, A. H. Safavi-Naeini, F. Marsili, M. D. Shaw, and O. Painter, Nature (London) **520**, 522 (2015).
[23] F. Lecocq, J. D. Teufel, J. Aumentado, and R. W. Simmonds, Nat. Phys. **11**, 635 (2015).
[24] V. B. Braginsky, Y. I. Vorontsov, and K. S. Thorne, Science **209**, 547 (1980).
[25] V. B. Braginsky and F. Y. Khalili, Reviews of Modern Physics **68**, 1 (1996).
[26] J. B. Hertzberg, T. Rocheleau, T. Ndukum, M. Savva, A. A. Clerk, and K. C. Schwab, Nat. Phys. **6**, 213 (2010).
[27] J. Suh, A. J. Weinstein, C. U. Lei, E. E. Wollman, S. K. Steinke, P. Meystre, A. A. Clerk, and K. C. Schwab, Science **344**, 1262 (2014).
[28] J. Suh, A. J. Weinstein, and K. C. Schwab, Appl. Phys. Lett. **103** (2013).
[29] J. Suh, M. D. Shaw, H. G. LeDuc, A. J. Weinstein, and K. C. Schwab, Nano Lett. **12**, 6260 (2012).
[30] See Supplemental Material,which includes Ref. [36].
[31] M. J. Woolley and A. A. Clerk, Phys. Rev. A **87**, 063846 (2013).
[32] M. J. Woolley and A. A. Clerk, Phys. Rev. A **89**, 063805 (2014).
[33] S. L. Braunstein and P. van Loock, Rev. Mod. Phys. **77**, 513 (2005).
[34] W. H. Zurek, Phys. Today **44**, 36 (1991).
[35] B. L. Hu and Y. Zhang, Mod. Phys. Lett. A **08**, 3575 (1993).
[36] R. Andrews, A. Reed, K. Cicak, J. Teufel, and K. Lehnert, Nat. Commun. **6**, 10021 (2015).

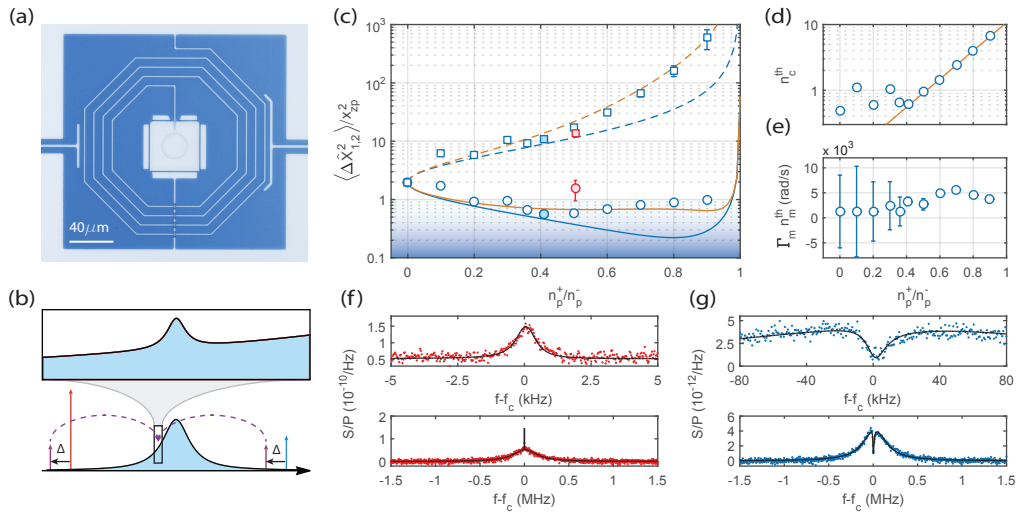


FIG. 1. (a) Optical micrograph of the device. The gray region is aluminum, the blue region is silicon. The square at the center is a parallel plate capacitor which is coupled to a spiral inductor to form a microwave resonator. The top gate of the capacitor is a compliant membrane whose fundamental motion is being studied. (b) Schematic of the pumps (red and blue arrows) and probes (purple arrows) relative to the cavity resonance. The inset shows the schematic of the BAE probe sideband spectrum. (c) The squeezed quadrature variances (circles) and anti-squeezed quadrature variances (squares) inferred from the output spectra. The red (blue) symbols represent the squeezed states achieved at $n_p^{\rm tot} = 1.35 \times 10^4$ ($n_p^{\rm tot} = 1.85 \times 10^5$). The blue shaded region indicates sub-zero point squeezing. The blue curves are the predictions from Eq. (4) with constant cavity and mechanical occupations at $n_p^+/n_p^- = 0$. The orange curves are the predictions from Eq. (4) including cavity heating effect extracted from the experiment. (d) The cavity occupation $n_c^{\rm th}$ extracted from the output spectrums, the orange line is a linear fit of the pump ratio dependent heating. (e) The phonon bath heating rate $\Gamma_m n_m^{\rm th}$ extracted from the output spectrums. (f) (g) The output spectra normalized by the transmitted power of the red-detuned pump. The upper inset is the normalized noise spectrum of the mechanical sideband, the lower inset is the noise spectrum of the cavity resonance. (f) The normalized output spectra correspond to the solid red circle in Fig. 1c. (g) The normalized output spectra correspond to the solid blue circle in Fig. 1c.

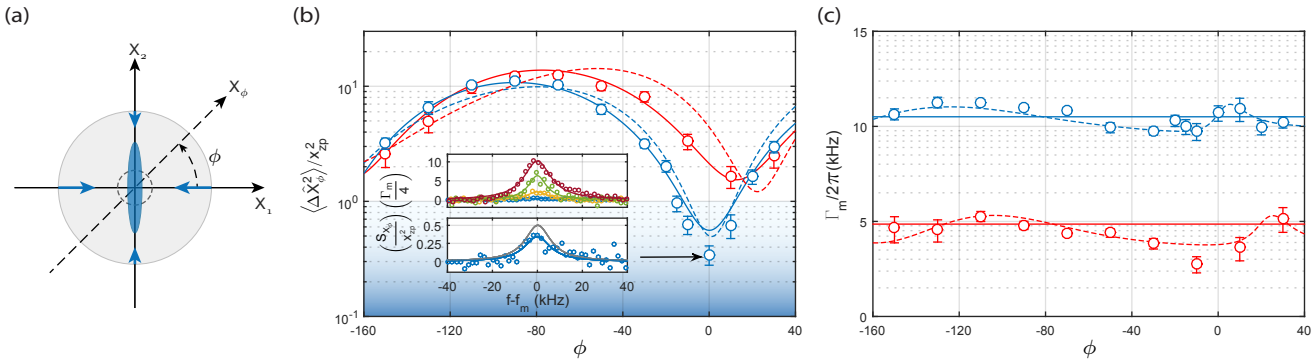


FIG. 2. (a) Schematic of dissipative mechanical squeezing. The gray circle represents the initial thermal state in phase space. The engineered reservoir generates phase dependent dissipation that relaxes the mechanics into a squeezed state, which is represented by the blue ellipse. The gray dashed circle represents the zero-point level. (b) Mechanical quadrature variance as a function of probe phase. The blue shaded region indicates sub-zero point squeezing. The red (blue) circles are the quadrature variances of the weakly (strong) squeezed state as measured using the BAE technique. The solid curves are the quadrature variances inferred from the corresponding output spectra assuming no mechanical parametric drive. The dashed curves are the predictions of an optomechanical model including the mechanical parametric effect. The insets are the mechanical quadrature spectra of the strong squeezed state with phase $\phi$ at $-70°$ (red), $-50°$ (green), $-20°$ (yellow), $0°$ (blue). The gray Lorentzian in the lower inset represents the spectrum with quadrature variance equal to half of the zero-point fluctuation (the 3 dB limit). (c) Mechanical quadrature linewidth as a function of probe phase. The red (blue) circles are the measured mechanical quadrature linewidth of the weakly (strong) squeezed state. The solid lines are the theoretical predictions from the ideal optomechanical model. The dashed curves are the fit with the optomechanical model including the mechanical parametric interaction.